

Relativistic axions from collapsing Bose stars

D.G. Levkov,^{1,*} A.G. Panin,^{1,2} and I.I. Tkachev¹

¹*Institute for Nuclear Research of the Russian Academy of Sciences,
60th October Anniversary prospect 7a, Moscow 117312, Russia*

²*Moscow Institute of Physics and Technology, 141700, Dolgoprudny, Russia*

The substructures of light bosonic (axion-like) dark matter may condense into compact Bose stars. We study collapses of the critical-mass stars caused by attractive self-interaction of the axion-like particles and find that these processes proceed in an unexpected universal way. First, nonlinear self-similar evolution (called “wave collapse” in condensed matter physics) forces the particles to fall into the star center. Second, interactions in the dense center create an outgoing stream of mildly relativistic particles which carries away an essential part of the star mass. The collapse stops when the star remnant is no longer able to support the self-similar infall feeding the collisions. We shortly discuss possible astrophysical and cosmological implications of these phenomena.

1. Introduction. Increasingly stringent experimental constraints [1] on low-energy supersymmetry reignited discussion of non-supersymmetric dark matter candidates such as the QCD axion [2] and axion-like particles (ALP) [3]. The interest is heated up by fast progress [4] in ALP searches and peculiar properties of the axion-like dark matter related, in particular, to the misalignment mechanism of its generation [5], see also [6, 7].

A very special possibility opening up due to tiny velocities and large occupation numbers of the ALP dark matter is formation of Bose stars [8–10] — gravitationally bound puddles of the ALP Bose condensate. These objects were observed as “solitonic galaxy cores” in numerical simulations [11] of structure formation by ultralight ($m \sim 10^{-22}$ eV) ALP dark matter. At larger ALP masses and, notably, in the case of the QCD axion, the Bose stars were conjectured [6, 12] to appear in the centers of the axion miniclusters [13, 14] which populate the Universe if the Peccei-Quinn symmetry is broken after inflation, cf. [15]. Although the last mechanism is not yet confirmed by numerical modeling, it is safe to say that the axion Bose stars constitute a part of the dark mass at least in some ALP dark matter models.

Rich phenomenology of the Bose stars is related to the peculiar self-interaction potentials [2, 3] of the ALP and QCD axion fields $a(x)$,

$$\mathcal{V} = m^2 f_a^2 (\theta^2/2 - g_4^2 \theta^4/4! + \dots), \quad \theta \equiv a/f_a, \quad (1)$$

which contain, besides the mass m , interaction terms suppressed by the new physics scale f_a . Typically, $\mathcal{V}(\theta)$ is periodic and the quartic constant $\lambda_4 \equiv -g_4^2 m^2/f_a^2$ is negative. This introduces attraction between the ALP and causes [9] collapse of large-mass Bose stars which previously was studied in [16, 17] using the Gaussian Ansatz.

In this Letter we present full field-theoretical study of the collapse. We reveal for the first time its complete dynamics and show that it leads to explosions of the Bose stars. First, the star Bose condensate undergoes “wave collapse” [18, 19]. Namely, it approaches a singular density profile due to self-similar infall of the ALP into the star center. Second, multiparticle relativistic interactions

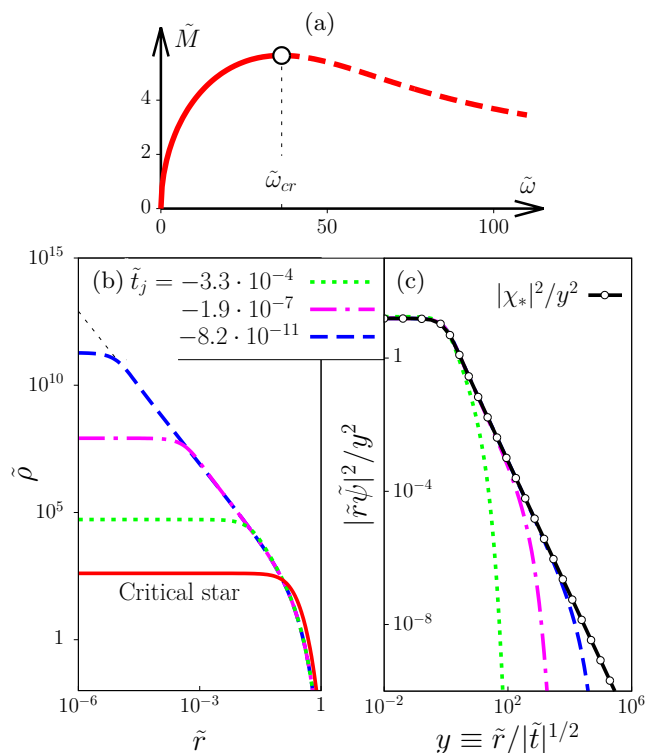


FIG. 1. (a) Star mass as a function of the binding energy $\tilde{\omega}$. (b) Numerical solution $\tilde{\rho} \equiv |\tilde{\psi}(\tilde{t}_j, x)|^2$ at fixed time moments \tilde{t}_j approaching $\tilde{t}_* \equiv 0$. (c) The same solution in the self-similar coordinates versus the asymptotic profile $\chi_*(y)$.

in the dense center produce an outgoing stream of mildly relativistic ALP. These two processes repeat many times.

2. Nonrelativistic evolution. Substituting the Ansatz $a/f_a = \sqrt{2} \operatorname{Re}(\psi e^{-imt})$ into the classical field equation and making the standard small-field and small-velocity assumptions, one obtains the nonrelativistic Gross-Pitaevskii-Poisson equations [9, 10],

$$i\partial_t \psi = -\Delta \psi/2m + m(\Phi - g_4^2 |\psi|^2/8) \psi, \quad (2)$$

$$\Delta \Phi = 4\pi\rho/M_{pl}^2, \quad (3)$$

which incorporate gravitational and quartic ALP interactions; $\Phi(t, \mathbf{x})$ and $\rho = m^2 f_a^2 |\psi|^2$ are the gravitational potential and ALP mass density, respectively. Note that all physical constants disappear from Eqs. (2), (3) after coordinate and field rescaling: $t = \tilde{t}/mv_0^2$, $x = \tilde{x}/mv_0$, $\psi = v_0 \tilde{\psi}/g_4$ and $\Phi = v_0^2 \tilde{\Phi}$, where $v_0 \equiv f_a/g_4 M_{pl} \ll 1$. This gives universal description of nonrelativistic evolutions at essentially different values of parameters.

Nonrelativistic Bose stars [8–10] are stationary spherically-symmetric solutions to Eqs. (2), (3) of the form $\psi = \psi_s(r) e^{-i\omega t}$, $\Phi = \Phi_s(r)$, where ω and ψ_s are the binding energy and wave function of the condensate particles, r is the radial coordinate. We numerically find the family of Bose stars parametrized with $\tilde{\omega} \equiv \omega/(mv_0^2)$; their mass $\tilde{M}(\tilde{\omega})$ is plotted in Fig. 1a.

The star mass is maximal at some critical value $\tilde{\omega} = \tilde{\omega}_{cr}$: $M_{cr} \equiv M(\tilde{\omega}_{cr}) \approx 10.2 f_a M_{pl}/mg_4$. This result was first obtained in [9]. The stars with $\tilde{\omega} > \tilde{\omega}_{cr}$ are unstable: they violate the necessary Vakhitov-Kolokolov criterion $dM/d\omega > 0$ [18, 20]. Physically, this instability is caused by the attractive g_4 -interaction which wins over quantum pressure and causes the stars to collapse. This reveals the fate of the Bose stars in the Universe: they form, grow overcritical by condensing the ALP, and finally collapse.

Now, consider the last stage of the star lifetime, i.e. the collapse. We compute the critical star profile $\psi = \psi_s(r)$ at $\tilde{\omega} = \tilde{\omega}_{cr}$, then slightly increase its mass by transforming $\psi_s(r) \rightarrow \gamma \psi_s(\gamma r)$ with $\gamma = 1 - 10^{-4}$. We numerically evolve the resulting overcritical configuration [21] by solving Eqs. (2), (3) in spherical symmetry. The numerical solution $\tilde{\rho} = |\tilde{\psi}(\tilde{t}_j, \tilde{r})|^2$ is shown in Fig. 1b at consecutive non-uniformly spaced time moments \tilde{t}_j . At first, the star is thin and wide, and well described by the Gaussian profile [16, 17]. Then the profile changes and a central singularity $|\psi| \propto r^{-1}$ at $t = t_*$ appears; we set $t_* = 0$ without loss of generality [22]. Spontaneous appearance of singularities is a nonlinear wave phenomenon called “wave collapse” in condensed matter physics [18, 19]. It is nontrivial and always related to strongly singular attractive potentials like $\Delta U \propto -|\psi|^2$ in the last term of Eq. (2) with $|\psi|^2 \propto r^{-2}$.

3. Self-similar solution. To describe the wave collapse analytically, we ignore the gravitational potential $m\Phi \ll \Delta U$ at small r . After that we can use results of Ref. [18]. Equation (2) acquires a continuous two-parametric scaling symmetry $\psi(t, x) \rightarrow \gamma \psi(\gamma^2 t, \gamma x) e^{i\alpha}$ and hence the scale-invariant solution $\psi = (-mt)^{-i\omega_*} \chi_*(y)/mrg_4$, where $y = r\sqrt{-m/t}$ is the self-similar coordinate and $\chi_*(y)$ satisfies the equation

$$-2\omega_* \chi + iy \partial_y \chi = -\partial_y^2 \chi - |\chi|^2 \chi / 4y^2 \quad (4)$$

following from Eq. (2). We numerically solve Eq. (4) with finite-energy boundary conditions $\chi_*(0) = 0$ and $\chi_* \rightarrow \chi_0 y^{-2i\omega_*}$ as $y \rightarrow +\infty$. We find a unique solution with

parameters $\omega_* \approx 0.54$ and $\chi_0 \approx 2.85$ shown in Fig. 1c by black line with open dots.

Solution of Eq. (4) was extensively discussed in condensed matter physics, see [18]. Here we demonstrate that χ_* is an attractor of the Bose star collapse. Indeed, the central part of the rescaled numerical solution $\tilde{r} \tilde{\psi}(\tilde{t}_j, \tilde{r})$ in Fig. 1c approaches χ_* as $\tilde{t}_j \rightarrow \tilde{t}_*$. At finite r and $t \rightarrow t_* \equiv 0$ one finds $y \rightarrow +\infty$. Thus,

$$g_4 \psi(t_*, r) = \chi_0 \cdot (mr)^{-2i\omega_* - 1} + \psi_{reg}(r), \quad (5)$$

where we separated the large- y asymptotic of χ_* and denoted the periphery part of the solution as $\psi_{reg}(r)$, cf. [18]. The small- r behavior of $\psi(t_*, r)$ is given by the first term in Eq. (5) which is *universal* i.e. does not depend on the initial conditions. Departures from the universality at large mr are described by $\psi_{reg}(r)$.

We numerically checked that the wave collapse occurs beyond spherical symmetry. To this end we added an axially-symmetric perturbation $\delta\psi/\psi \sim 10^{-2}$ to the critical star and evolved the resulting configuration with the axially-symmetric code. We obtained the solution approaching the same spherically-symmetric attractor χ_* and, eventually, the singular profile (5).

4. Relativistic evolution. The nonrelativistic equations (2), (3) are not applicable in the vicinity of the central singularity at $t \sim t_*$. First, the ALP velocities $v \sim \partial_r \psi / m\psi \sim -(mr)^{-1}$ in the configuration (5) exceed the speed of light at $mr \lesssim 1$. Second, the small-field approximation $\psi \sim a/f_a \ll 1$ breaks down in the same region, and the higher-order terms of the potential (1) become important. We expect that the condensate flow down the potential well should stop at $mr \lesssim 1$ and $t \approx t_*$ because the full ALP potential \mathcal{V} is bounded from below. Instead, relativistic collisions in the dense center should produce a stream of relativistic axions escaping the star.

We study evolution of the Bose star at $t \gtrsim t_*$ by solving numerically the spherically-symmetric relativistic field equation,

$$f_a \square a = -(1 + 2\Phi) \mathcal{V}'(a/f_a), \quad (6)$$

with the full scalar potential \mathcal{V} . For definiteness, in what follows we consider the potential of the QCD axions [23]

$$\mathcal{V} = m^2 f_a^2 z^{-1} (1+z) \left(1+z - \sqrt{1+z^2 + 2z \cos \theta} \right) \quad (7)$$

with $z \equiv m_u/m_d \approx 0.56$, although the other bounded potentials produce similar results. The quartic constant in Eq. (1) is now fixed: $g_4^2 = (1+z^2 - z)/(1+z)^2$.

Note that Eq. (6) still involves the nonrelativistic gravitational potential Φ satisfying Eq. (3) with $\rho = (\partial_t a)^2/2 + (\partial_r a)^2/2 + \mathcal{V}$. This is legitimate: departures from the Newtonian gravity occur only in the region $mr \lesssim 1$ where it has negligible effect on solution, see (5).

After finding the numerical solution of Eqs. (6), (3), we plot the energy density in the star center $\rho(t, 0)$ in

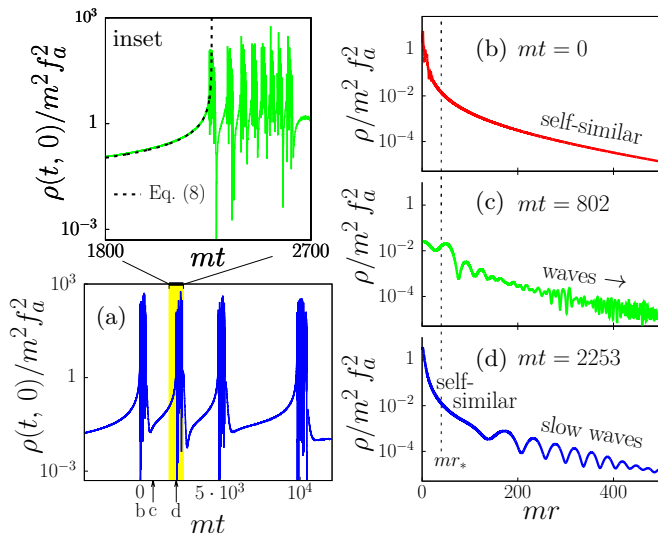


FIG. 2. (a) The central energy density $\rho(t, 0)$ of the collapsing star with $f_a^2 = 5 \cdot 10^{-8} M_{pl}^2$. The region corresponding to the second explosion is magnified in the inset. (b), (c), (d) The density profiles $\rho(t, r)$ of this star at fixed t .

Fig. 2a. One observes that the initial self-similar growth of the density at $t < t_* = 0$ leads to an “explosion” — a period of violent oscillations at $t \approx 0$ accompanied by strong emission of the outgoing high-frequency waves in Figs. 2b,c, see Supplemental Material for the movie. The oscillations are governed by nonlinear interaction [24] of the relativistically infalling condensate at $mr \lesssim 1$. In terms of particle physics this is a relativistic collision of many condensate particles in the star center producing an outgoing flux of relativistic ALP. The particle number is strongly violated in this process.

The outgoing relativistic flux rapidly makes the star center diluted. Then after the first explosion the process repeats itself: the central density starts to grow until the second period of violent oscillations occurs, etc, see Figs. 2a,c,d. To explain this behavior, we recall that the self-similar solution studied above is the attractor of the nonrelativistic evolution. This means that the nonrelativistic condensate outside of the diluted core should once again develop the universal singular profile (5) as $t \rightarrow t'_*$. We support this observation by noting that the central energy density of the self-similar solution $|\psi| = |\chi_*(y)|/mrg_4$ behaves as

$$\rho(t, 0)/m^2 f_a^2 = |\partial_y \chi_*(0)|^2 / [g_4^2 m (t'_* - t)], \quad (8)$$

with $\partial_y \chi_*(0) \approx 3.99$. In the inset of Fig. 2a we demonstrate that the function $\rho(t, 0)$ at the eve of the second explosion is well fitted by Eq. (8) (shown by the dashed line) with one adjustable parameter t'_* . We conclude that the collapsing star indeed repeatedly develops singular profiles (5) triggering scattering of the relativistic ALP in the star center.

5. *Emission spectrum.* Since the wave collisions in the star center always start from the approximately uni-

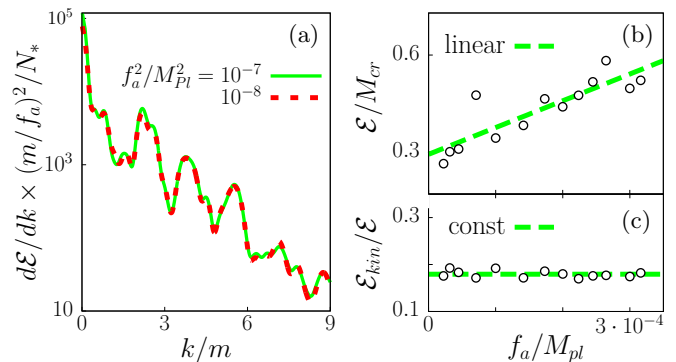


FIG. 3. (a) The spectra $d\mathcal{E}/dk$ of emitted particles per one explosion. The graphs are averaged over the sensitivity intervals $\delta k = 0.1 m$ for visualization purposes. (b), (c) The portion of mass \mathcal{E}/M_{cr} leaving the collapsing star during its full lifetime and the fraction of kinetic energy $\mathcal{E}_{kin}/\mathcal{E}$ within the outgoing particle stream as functions of the ALP scale f_a .

versal initial data (5), their dynamics and the spectra of the emitted ALP are almost the same. To calculate the spectra, we consider the spherical axion waves freely propagating away from the star at large r : $a(t, r) \approx \text{Re} \int_0^{+\infty} dk A_k e^{ikr - i\omega_k t} / r$, where $\omega_k^2 = k^2 + m^2$. We numerically compute the wave amplitudes A_k using the time Fourier transforms of the field $a(t, R)$ and its derivative $\partial_r a(t, R)$ at large $r = R$. Then the spectrum or, more exactly, the distribution of the total emitted energy \mathcal{E} over the momenta k of the outgoing particles, is $d\mathcal{E}/dk = 4\pi^2 \omega_k^2 |A_k|^2$.

In Fig. 3a we plot the spectra emitted by two collapsing stars, each divided by the number of explosions during the collapse N_* . The spectra are wide, with several almost equidistant peaks — these may appear due to multiple re-scattering of the outgoing ALP off the infalling condensate [25]. The two graphs in Fig. 3a coincide although the respective processes proceed at essentially different f_a and involve $N_* = 3$ and 7 explosions. This confirms that the explosions are identical: the total spectrum is given by the one in Fig. 3a multiplied by N_* .

However, the number of explosions N_* and therefore the total emitted energy \mathcal{E} depend on the potential \mathcal{V} . Figure 3b shows that \mathcal{E} is an almost linear function of f_a/M_{pl} . Extrapolating it to phenomenologically relevant values $f_a \ll M_{pl}$, we find that the collapsing stars in the model (7) lose roughly 30% of their mass, $\mathcal{E} \sim 0.3 M_{cr}$.

6. *Discussion.* To summarize, the Bose star collapse involves two alternating processes: the self-similar evolution approaching the singular profile (5) and ALP scattering in the star center accompanied by strong emission of relativistic particles. The first process is described, after the appropriate field and coordinate rescalings, by the universal nonrelativistic solution. The subsequent scattering, although non-universal by itself [26], starts from the universal profile (5) at each cycle and therefore pro-

duces the same outgoing flux of the axion-like particles. The collapse stops when the star remnant is not able to support the self-similar evolution. We numerically checked that the remnant is gravitationally bound. It may therefore settle into a subcritical star, which, if surrounded by the ALP minicluster, may again grow overcritical by condensing the axions and collapse.

Note that contrary to the recent suggestion [16] the collapsing star does not form a black hole at $f_a \lesssim M_{pl}$ because the central region of the configuration (5) in this case remains outside of its gravitational radius. On the other hand, black hole formation is expected [27] at $f_a \gtrsim M_{pl}$.

Our results essentially modify cosmology and astrophysics of the ultralight ALP with $m \sim 10^{-22}$ eV and relatively low ALP scale $f_a < 10^{15}$ GeV. In this case the largest masses $M \sim 10^9 M_\odot$ of the Bose stars observed in the full-scale simulation [11] are above M_{cr} . The collapse of those stars into relativistic ALP with spectrum in Fig. 3a should radically change the model predictions once the self-coupling is taken into account.

Application of our results to other ALP models depends on whether their Bose stars populate the Universe or not. In the particular case of the QCD axions with $m \sim 10^{-4}$ eV the value of the critical mass $M_{cr} \sim 10^{-13} M_\odot$ is somewhat smaller than the typical mass of the axion miniclusters. If the conjecture of [6] is valid and the miniclusters condense into Bose stars, the latter should eventually collapse ruining the former and producing the relativistic axions. This is important for observations [28]. Another possible application is emission, during the collapse, of radio waves which may be directly observable [29]. Their specific time pattern related to Fig. 2 and widening of their spectrum due to relativistic axion velocities in the star core, cf. Fig. 3a, may serve as distinctive signatures of the star collapse.

Prominent cosmological phenomena should appear in very special ALP dark matter models where Bose stars carry a considerable fraction of the dark mass at some stage of the Universe evolution, cf. [15, 30]. Indeed, the collapse turns 30% of the total mass of overcritical stars into warm dark matter with universal spectrum in Fig. 3a containing 18% of kinetic energy, see Figs. 3b,c. The net effect of this process on the structure formation and cosmological parameters should be similar to that of the dark matter decaying into dark radiation [31].

We thank E. Nugaev and S. Sibiryakov for discussions. This work was supported by the grant RSF 16-12-10494. Numerical calculations were performed on the Computational cluster of the TD INR RAS.

* levkov@ms2.inr.ac.ru

[1] K. A. Ulmer [CMS and ATLAS Collaborations],

arXiv:1601.03774.

- [2] P. Sikivie, Lect. Notes Phys. **741**, 19 (2008). J. E. Kim and G. Carosi, Rev. Mod. Phys. **82**, 557 (2010).
- [3] A. Arvanitaki *et al.*, Phys. Rev. D **81**, 123530 (2010).
- [4] P. W. Graham *et al.*, Ann. Rev. Nucl. Part. Sci. **65**, 485 (2015).
- [5] J. Preskill, M. B. Wise and F. Wilczek, Phys. Lett. B **120**, 127 (1983). L. F. Abbott and P. Sikivie, Phys. Lett. B **120**, 133 (1983). M. Dine and W. Fischler, Phys. Lett. B **120**, 137 (1983). P. Arias *et al.*, JCAP **1206**, 013 (2012).
- [6] E. W. Kolb and I. I. Tkachev, Phys. Rev. Lett. **71**, 3051 (1993); Phys. Rev. D **49**, 5040 (1994).
- [7] O. Wantz and E. P. S. Shellard, Phys. Rev. D **82**, 123508 (2010). T. Hiramatsu *et al.*, Phys. Rev. D **85**, 105020 (2012) [*Erratum-ibid.* **86**, 089902 (2012)]. M. Kawasaki, K. Saikawa and T. Sekiguchi, Phys. Rev. D **91**, 065014 (2015).
- [8] R. Ruffini and S. Bonazzola, Phys. Rev. **187**, 1767 (1969). I. I. Tkachev, Sov. Astron. Lett. **12**, 305 (1986).
- [9] P. H. Chavanis, Phys. Rev. D **84**, 043531 (2011). P. H. Chavanis and L. Delfini, Phys. Rev. D **84**, 043532 (2011).
- [10] J. Eby *et al.*, JHEP **1602**, 028 (2016).
- [11] H.-Y. Schive, T. Chiueh and T. Broadhurst, Nature Phys. **10**, 496 (2014). H.-Y. Schive *et al.*, Phys. Rev. Lett. **113**, 261302 (2014).
- [12] E. Seidel and W. M. Suen, Phys. Rev. Lett. **72**, 2516 (1994).
- [13] C. J. Hogan and M. J. Rees, Phys. Lett. B **205**, 228 (1988). E. W. Kolb and I. I. Tkachev, Phys. Rev. D **50**, 769 (1994).
- [14] E. Hardy, arXiv:1609.00208.
- [15] A. H. Guth, M. P. Hertzberg and C. Prescod-Weinstein, Phys. Rev. D **92**, 103513 (2015).
- [16] P.-H. Chavanis, arXiv:1604.05904.
- [17] J. Eby *et al.*, arXiv:1608.06911.
- [18] V. E. Zakharov and E. A. Kuznetsov, Phys. Usp. **55**, 535 (2012) and references therein.
- [19] E. A. Donley *et al.* Nature **412**, 295 (2001).
- [20] N. G. Vakhitov and A. A. Kolokolov, Radiophys. Quantum Electron. **16**, 783 (1971).
- [21] We use nonuniform lattice with adaptive refinement, Kreiss-Oliger dissipation, the second-order iterated Crank-Nicholson integrator for the nonrelativistic evolution and the sixth-order Runge-Kutta method for the relativistic one. These advanced numerical techniques are targeted at achieving record precision of the numerical solution which starts from 10^{-10} in the beginning of the collapse and degrades to 10^{-2} at $mt \sim 10^4$.
- [22] The collapse time $t_{coll} \propto 1/mv_0^2$ was considered in [16].
- [23] G. Grilli di Cortona *et al.*, JHEP **1601**, 034 (2016).
- [24] During these oscillations the field amplitude at $r = 0$ exceeds $2\pi f_a$ which may be loosely interpreted as a formation of short-living axion domain wall surrounding the star center.
- [25] S. Yu. Khlebnikov and I. I. Tkachev, Phys. Rev. Lett. **77**, 219 (1996).
- [26] The qualitative features of the spectrum, however, are model-independent. We confirmed this by performing calculations for $\mathcal{V} = m^2 f_a^2 (1 - \cos \theta)$ and the potential with $\theta^6/6!$ in place of dots in Eq. (1). In both cases the spectrum was mildly relativistic with several wide peaks.
- [27] When this Letter was under review, a confirmation ap-

- peared, see T. Helfer *et al.*, arXiv:1609.04724.
- [28] P. Tinyakov, I. Tkachev and K. Zioutas, JCAP **1601**, 035 (2016).
- [29] I. I. Tkachev, JETP Lett. **101**, 1 (2015).
- [30] S. Davidson and T. Schwetz, Phys. Rev. D **93**, 123509 (2016).
- [31] B. Audren *et al.*, JCAP **1412**, 028 (2014). A. Chudaykin, D. Gorbunov and I. Tkachev, Phys. Rev. D **94**, 023528 (2016).